

Experimental and Numerical Research on Hysteretic Behaviors of Tubular Reinforced Concrete Columns

Yazhou Xu¹

¹ *Ph. D candidate, Department of Building Engineering, Tongji University, Shanghai, China
Email: yazhou.xhu@gmail.com*

ABSTRACT:

The behavior of tubular reinforced concrete columns (TRCC) under cyclic loading is experimentally and numerically investigated. Firstly, four specimens 1/8 of the prototype column are fabricated and tested. In this paper, the hysteretic loops are analyzed just for two specimens, namely tube 1 and tube 3. Then the skeleton curves and hysteretic loops of TRCC are simulated by FEM programming ABAQUS. With suitable selection of the constitutive models for concrete and their parameters, the FEM models can capture the main features of TRCC subjected to monotonic and cyclic loading. Finally, based on the numerical results, the influence of axial compression ratio on the ultimate load is studied. It is confirmed that increasing axial compression ratio is adverse to the seismic performance of TRCC. Both the experimental and numerical results show that TRCC exhibit a moderate ability of energy dissipation.

KEYWORDS: reinforced concrete tubular column, hysteretic behavior, loops, cyclic loading

1. INTRODUCTION

Hysteretic behavior is an important concept in structural engineering, especially for aseismatic structures. It reflects the ability of energy dissipation and collapse resistance of a structure at different levels, such as material, member and structure as a whole. Numerical and experimental investigations of reinforced concrete members subjected to cyclic loadings have undergone for many years. And lots of research papers and reports have been published (Nilsson and Arthur H., 1968, Bathe K.J. and Ramaswamg S., 1979) . It has been found that hysteretic behaviors of reinforced concrete members strongly depend on section shape, slender ratio, material property, axial compression ratio, reinforcement ratio, detailing art, stirrups, and so on.

With the fast development of modeling skills and computer technology, great progress has been made (Elmorsi M., 1998, Yashiaki Goto, 1998, Lee J., 1999, Feenstra P.H., 2000, W.-P. Kwan, 2001, Hyo-Gyoung Kwak, 2001) since Ngo and Scordelis (1967) firstly used the nonlinear finite element method (FEM) to simulate reinforced concrete members. But few

papers on numerical simulations of hysteretic properties of TRCC are available, although TRCC are widely used in buildings and bridges, particularly for industrial facilities. Wang et al (2004) carried out an experiment to study six high strength concrete tubular columns subjected to axially compressive and tensile loading. The influences of compressive strength of concrete and slender ratio of columns on the ultimate bearing capacity are analyzed numerically. Masukawa Junji, Suda Kumiko and Maekawa Koichi (1999) investigated hollow bridge piers considering concrete cover spalling and steel buckling by three-dimensional nonlinear finite element method.

In this paper, the hysteretic properties of TRCC are experimentally and numerically studied. Four specimens 1/8 of the prototype column are fabricated and tested under the combined vertical compression and horizontal cyclic loading. Commercial FEM programming ABAQUS are employed to simulate the monotonic skeleton curves and hysteric loops for two specimens. Based on the verification of FEM models by the experimental results, axial compression ratio is taken as a parameter to numerically study its influence on the ultimate load. Compared with the experimental results, the numerical analysis can capture the main features of the hysteric behavior of TRCC.

Table 1 Details of specimens

Tubular columns	Diameter (mm)	Thickness (mm)	f_{cu} (MPa)	f_c (MPa)	Axial Force (kN)	Reinforcement (mm^2)
Tube1	500	50	38	18.2	180	1179
Tube3	500	50	34	16.2	344	1729

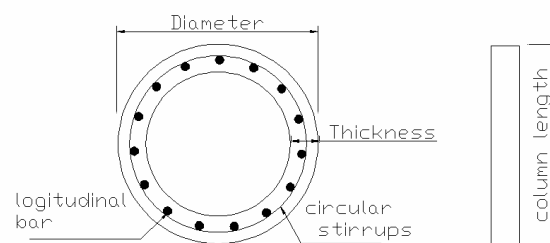


Fig. 1 Schematic diagram for notation of Table 1

2. Experiment and analysis of results

The prototype columns, used as the supporting piers of the air condenser in a thermal plant, are 24.6m tall, with the outer diameter of 4.0m and the internal diameters of 0.4m or 0.8m. Confined to the maximum height of the testing machine, four specimens with the scale of 1/8 are produced and tested to study the hysteric behavior of the columns. The specimens are 3.07m high with the outer diameter of 0.5m and the thickness of 0.05m or 0.1m. The specimen sections are designed according to Chinese code (GB50010-2002). For Tube1 and Tube3, 15 and 24 longitudinal steel bars with the diameter of 10mm are used, respectively. The circular stirrup is 8mm in diameter and arranged with the spacing of 200mm except for the top and bottom 500mm of the columns, in which the spacing is 100mm. The detailed

dimensions of the specimens and the material properties are listed in Table 1, where f_{cu} , f_c , t , A_s denote cubic compression strength of concrete, prism compression strength of concrete, wall thickness and longitudinal steel area, respectively. The nominal yield strength of steel reinforcement and circular stirrup are 360MPa and 235MPa. The elastic modulus for concrete is 3e4 MPa , for steel 2.06e5 MPa. The tensile strength of concrete, f_t , is calculated following $f_t = 0.26 f_{cu}^{2/3}$.

The specimens are tested in a close loop controlled testing machine (MTS). The experimental setup is shown in Fig. 2. A standard lateral loading procedure is used for these specimens. Firstly, the specified axial compression is applied on the top of the columns and kept constant. Then under the gradually increased horizontal displacement, the top of the columns moves backward and forward until the columns yield. Eventually, the recorded displacement when steel yielding is taken as the new displacement increment and the foregoing process continues until the post-yield capacity is less than 85% of the ultimate load. During the experiment, the cracking load and displacement, the yielding load and the corresponding drift are recorded.



Fig. 2 Experimental setup



Fig. 3 Crack pattern for Tube1

Fig.3 shows the crack pattern of Tube 1. At the initial loading stage, the first visible crack of Tube 1 occurs when the horizontal displacement of the column top reaches 4mm. With the displacement increasing to 11mm, the horizontal cracks at the column bottom propagate and interpenetrate. The first inclined crack subsequently appears corresponding to 25mm of the top displacement. Finally, the concrete cover of the bottom end spalls and the maximum top displacement reached 64mm (Fig.4). Fig. 5 and Fig. 6 show the experimental hysteretic curves for Tube1 and Tube3 respectively. It can be found from those figures that the experimental loops show typically hysteretic features of reinforced concrete columns, i.e. apparent pinching effects and degradations of strength and stiffness. For Tube3, the hysteretic curves exhibit severe asymmetry and the degradations of strength and stiffness owing to its higher axial compression ratio than one of Tube1.



Fig. 4 Crushed concrete at the bottom end of Tube1

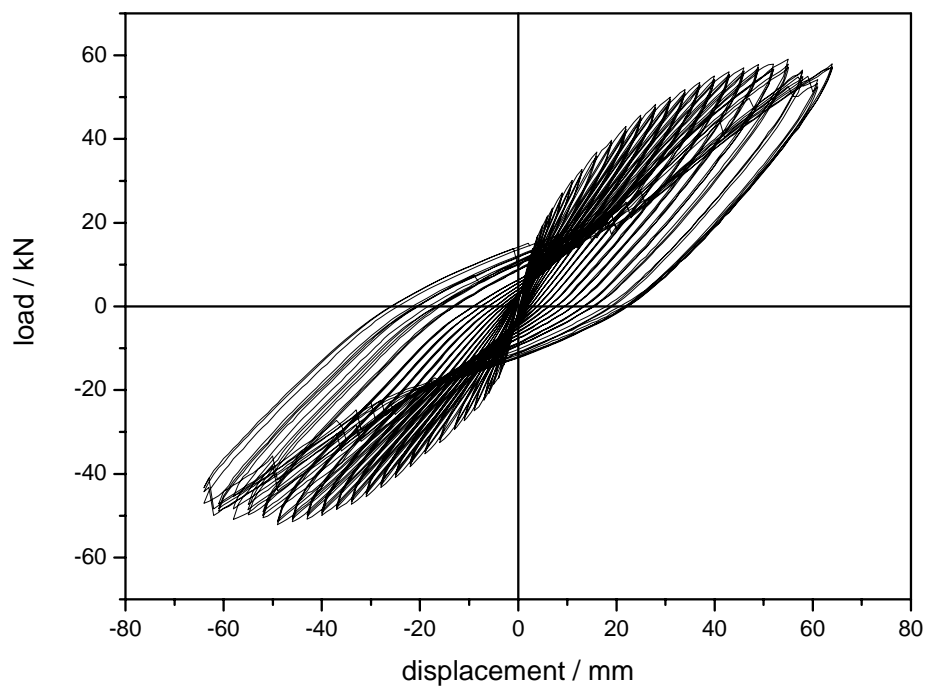


Fig. 5 Experimental hysteretic curves for Tube 1

3. Numerical simulation

Although nonlinear FEM for concrete structures have achieved significant progress since 1960s, to model hysteretic behaviors of concrete members correctly, there are still many

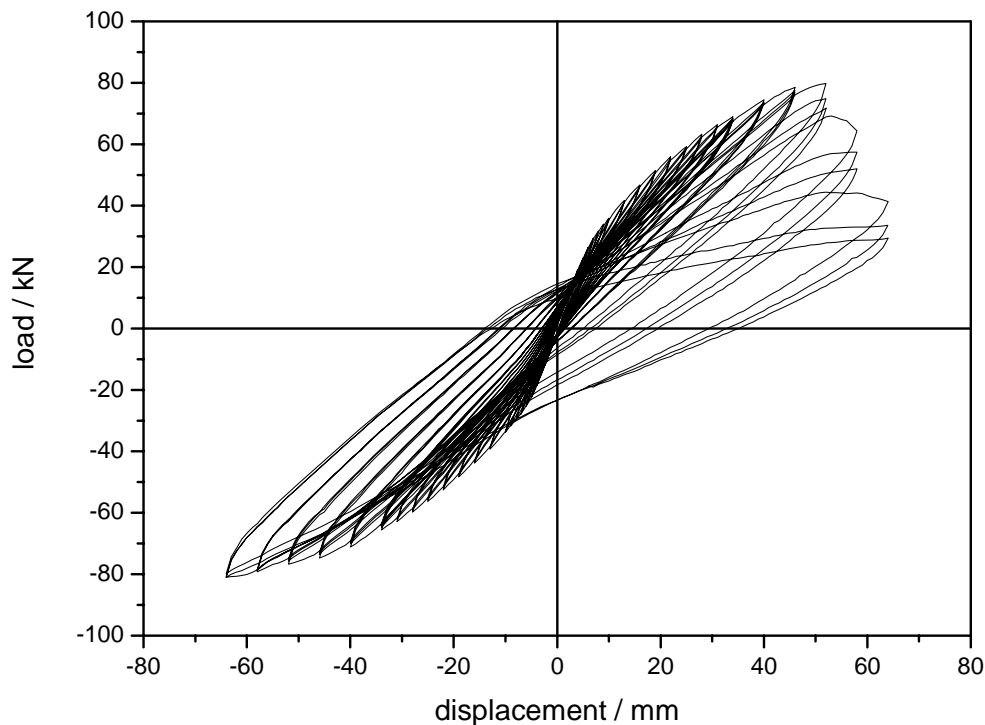


Fig. 6 Experimental hysteretic curves for Tube 3

challenges in material constitutive laws, FEM meshing skills, solution technology, computation efficiency, etc. Frankly speaking, no reasonable method can provide reliable simulation results for hysteretic loops until now. But for the ultimate bearing capacity, a good agreement with experimental results can be achieved based on careful selection of suitable material parameters, appropriate element type and meshing skill, efficient computation technology, and so on. In this study, the self-contained constitutive law in ABAQUS, plasticity smeared model and plasticity damage model, are chosen to model the behaviors of concrete subjected to monotonic and cyclic loading, respectively.

3.1 Monotonic loading

For the case of monotonic loading, the constitutive laws for concrete and steel are chosen as the plasticity smeared model and the perfect elasto-plastic model. The most important parameters of the plasticity smeared model are the stress-inelastic strain relation and the tensile stiffness of concrete. The former describes the compressive behaviors of concrete, while the latter reflects the tensile natures and the interaction between steel and concrete. Suitable selection of the tensile stiffness directly determines the convergence of the numerical simulation. Hognestad model is adopted as the compressive stress-strain relation for concrete. And linear strain-stress relationship is assumed for the tensile behavior of concrete. In this paper, Riks algorithm provided by ABAQUS is employed as the solution method.

Fig.7 shows the comparison of the experimental and numerical skeleton curves for Tube 1 and Tube 3. Good agreements can be found for both specimens. The experimental ultimate loads are 56.5kN and 78kN for Tube 1 and Tube 3, respectively. Correspondingly, the numerical results for the two tubular columns are 54.4kN and 71.1kN. However, the simulation displacement does not match the testing results very well. The main reason for this is that bond slip between steel and concrete, crack effects and concrete spalling are not considered. To investigate the influence of axial compression ratio on the ultimate load of columns, the magnitude of axial load is adjusted to compute the maximum load. The relationship between the axial compression ratio and the ultimate load is illuminated in Fig. 8. And the results under monotonic loading for Tube1 and Tube3 are shown in Fig. 9 and Fig. 10.

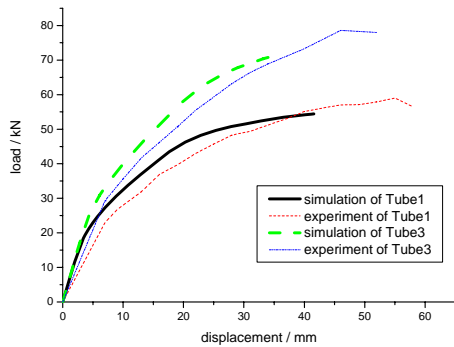


Fig. 7 Comparisons of the experimental and numerical skeleton curves

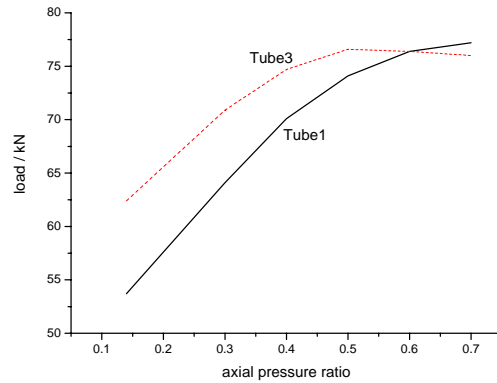


Fig. 8 The relationship between the axial compression ratio and the ultimate load

Obviously, with the increase of axial pressure ratio, the corresponding maximum load also increases. And when the axial pressure ratio reaches 0.6 and 0.7, the initial stiffness obviously decreases. For Tube3, the ultimate load starts to descend when the axial pressure ratio is over 0.5, due to its higher axial pressure ratio. Although owing to convergence difficulty, the numerical simulation terminates when the axial pressure ratio is larger than 0.7, it still can be found that the column under a higher axial load has a worse deformation capacity, which is unfavorable to seismic resistance.

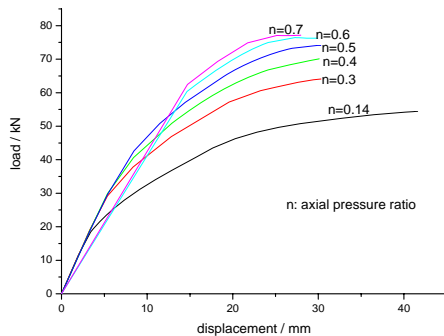


Fig. 9 Skeleton curves with different axial compression ratio for Tube1

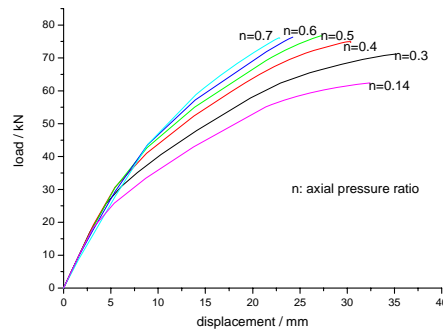


Fig. 10 Skeleton curves with different axial compression ratio for Tube3

3.2 Cyclic loading

It must be pointed out, owing to the intrinsic complexities such as constitutive relationship of concrete, bond-slip between steel and concrete, Bauschinger effect of steel, crack model, shear retention, material softening, and convergence of algorithm, the simulation for hysteretic curves is much more difficult and time-consuming than the skeleton curves under monotonic loading. In this paper, the constitutive law for concrete subjected to cyclic loading takes the plasticity damage model in ABAQUS, which provides compression damage coefficient, tension damage coefficient, compression recovery coefficient and tension recovery coefficient to take stiffness and strength degradation, shear transfer between cracks into consideration. In this plasticity damage model, the yielding criterion is defined by five parameters. Two of them are particularly noticeable. One is the dilation parameter which specifies the dilation angle in meridian plane at high confining pressure. Another is the ratio of the second stress invariant on the tensile meridian to the Mises equivalent effective stress on the compressive meridian, which regulates the shape of yielding surfaces on the deviatoric plane. FEM model and loading program are shown in Fig. 11.

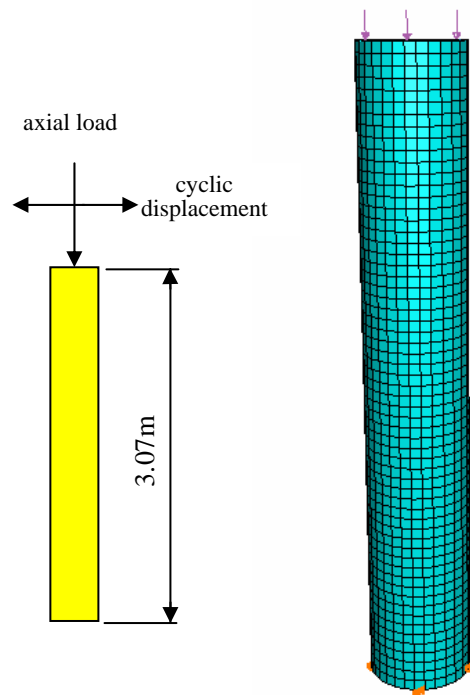


Fig. 11 Loading program (left) and FEM model (right)

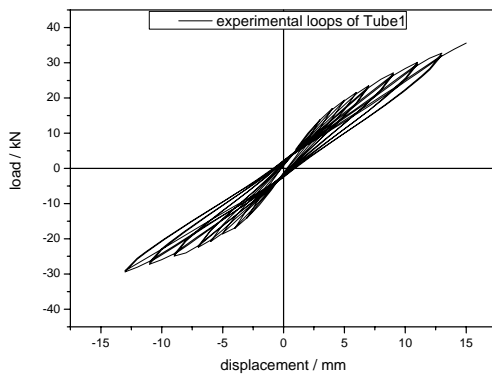


Fig. 12 Experimental loops for Tube1

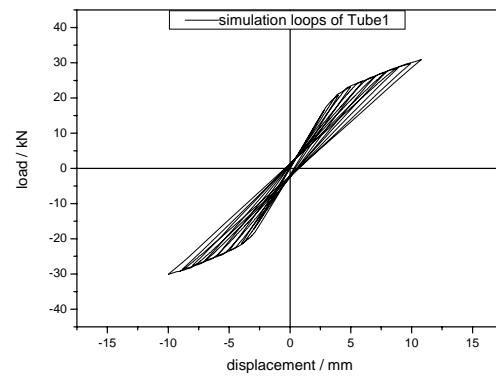


Fig.13 Simulation loops for Tube1

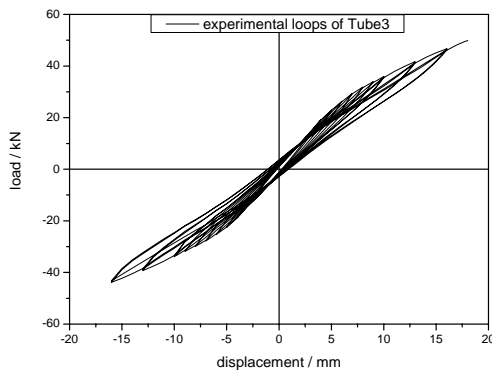


Fig. 14 Experimental loops for Tube3

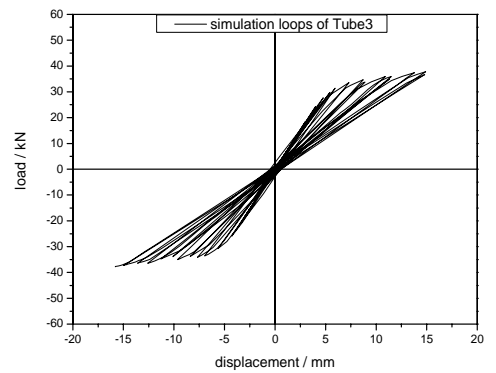


Fig.15 Simulation loops for Tube3

The simulation results of the hysteretic loops for Tube 1 and Tube 3 are plotted in Fig. 13 and Fig. 15. And corresponding test results are presented in Fig. 12 and Fig.14. From the comparison between the two results, it

can be found that as a whole this model can capture the main hysteretic features of concrete tubular columns, i.e., the stiffness degradation and the pinching effects. But the simulation results are more rigid than the test, and local shapes are not in a good agreement with experiment. The first reason is that this model does not include Bauschinger effects of steel and crack model of concrete. In fact, the numerical results are just the first several loops of the whole hysteretic curves. The second reason is, especially for softening branches, the convergence problem of the current numerical algorithm.

4. Summary and Conclusion

In this paper, the experimental program and results for two TRCC subjected to cyclic loadings are introduced. Hysteretic properties and seismic capacity are evaluated based on experimental and numerical results. Two columns, Tube1 and Tube3, are modeled by FEM programming ABAQUS to simulate their skeleton curves and loops. According to the experimental results, TRCC exhibit a moderate ability of energy dissipation, and their hysteretic loops show apparent pinching effects. The numerical results present that with the increase of the axial compression ratio, the ultimate load also increases at the initial stage. But when the axial pressure ratio exceeds a certain limit, the ultimate load displays a trend to decrease, and the initial stiffness also descends. Increasing the axial compression ratio, the degradation of strength and stiffness is more severe, just as loops of Tube 3 illuminates, which indicates a worse seismic performance.

Numerical models in ABAQUS can capture the main features of TRCC under both monotonic and cyclic loading. The plastic smeared model and plastic damage model can be used to simulate behaviors for structural concrete. The parameters in the two models provide a way to take account of shear transfer between cracks, degradation of strength and rigid, compressive softening and tensile stiffness in FEM models. The Riks algorithm has a better convergence than general static algorithm. The FEM results under monotonic loading have a good agreement with the test, but for cyclic loading it is hardly to simulate later steps of the experimental program. Further researches are needed on more accurate concrete models and better algorithm to improve the numerical prediction of the seismic behavior of TRCC.

REFERENCES

- ABAQUS User Manual. (2002), HKS, Inc.
- Bathe K.J. and Ramaswam S. (1979). On tree-dimensional nonlinear analysis of concrete structures. *Nuclear Engineering and design* **52:3**.
- Elmorsi, M., Kianoush, M. R. and Tso, W. K. (1998). Nonlinear analysis of cyclically loaded reinforced concrete structures. *ACI struct. J.* **95:6**, 725-39.
- Feenstra, P. H., and Rots, J. G. (2000). Comparison of concrete models for cyclic loading. *ASCE Workshop Proc.*, ASCE, Reston, Va., 38-55.
- GB50010-2002. (2002). Code for design of concrete structures.
- Kwak Hyo-Gyoung and Kim Sun-Pil. (2001). Nonlinear analysis of RC beam subjected to cyclic loading. *Journal of structural Engineering* **127 :12**, 1436-44.
- Junichi Sakai and Kazuhiko Kawashima. (2006). Unloading and reloading stress-strain model for confined concrete. *Journal of structural Engineering* **132 :1**, 112-22.
- Masukawa Junji, Suda Kumiko and Maekawa Koichi. (1999). Three-dimensional nonlinear FEM analysis of hollow bridge piers considering spalling of concrete cover and buckling of reinforcing bars. *Transactions of the Japan Concrete Institute* **21**, 255-262.
- Naser Mostaghel. (1999). Analytical description of pinching, degrading hysteretic systems. *Journal of Engineering Mechanics* **125 :2**, 216-24.
- Nilsson, Arthur H. (1968). Nonlinear analysis of reinforced concrete by the Finite Element Method. *ACI Journal* **65**.
- S. L. Billington and J. K. Yoon. (2004). Cyclic response of unbonded posttensioned precast columns with ductile fiber-reinforced concrete. *Journal of Bridge Engineering* **9:4**, 353-63.
- Yoshiaki Goto, Qingyun Wang and Makoto Obata. (1998). FEM analysis for hysteretic behavior of thin-walled



columns. *Journal of structural Engineering* **124 :11**, 1290-301.

Yutian Shao, Seyed Aval, and Amir Mirmiran. (2005). Fiber-Element Model for Cyclic Analysis of Concrete-Filled Fiber Reinforced Polymer Tubes. *Journal of structural Engineering* **131 :2**, 292-303.

Wang Guangyong, Sun Yongzhi, Fu Chuanguo, et al. (2004). Study and analysis on the mechanical behavior of high strength concrete tubular columns under axial load. *Journal of Shandong University of Architecture and Engineering* **19:1**, 12-16.

W. F., Chen. (1981). Plasticity on reinforced concrete, New York, McGraw-Hill Book Company, Inc.

W.-P., Kwan and S. L. Billington. (2001). Simulation of structural concrete under cyclic load. *Journal of structural Engineering* **127:12**, 1391-401.